

# Lawrence Berkeley National Laboratory

## Lawrence Berkeley National Laboratory

### Title

In/Si(111): Self-assembled one and two-dimensional electron gases

### Permalink

<https://escholarship.org/uc/item/9vp4j3hh>

### Authors

Rotenberg, Eli

Yeom, H.W.

Takeda, S.

et al.

### Publication Date

2001-01-22

## In/Si(111): Self-Assembled One and Two-Dimensional Electron Gases

Eli Rotenberg,<sup>2</sup> H. W. Yeom,<sup>6</sup> S. Takeda,<sup>1</sup> I. Matsuda,<sup>3</sup> K. Horikoshi,<sup>1</sup> J. Schaefer,<sup>4</sup> C. M. Lee,<sup>2</sup> B. Krenzer,<sup>4</sup> M. Rocha,<sup>4</sup> S. D. Kevan,<sup>4</sup> T. Ohta,<sup>3</sup> T. Nagao,<sup>1,5</sup> and S. Hasegawa<sup>1,5</sup>

<sup>1</sup>Department of Physics, the University of Tokyo, Tokyo 113-0033, Japan

<sup>2</sup>Advanced Light Source, Lawrence Berkeley National Laboratory, Berkeley, California 94720

<sup>3</sup>Department of Chemistry, the University of Tokyo, Tokyo 113-0033, Japan

<sup>4</sup>Department of Physics, University of Oregon, Eugene, Oregon 97403

<sup>5</sup>CREST, the Japan Science and Technology Corporation, Saitama 332-0012, Japan

<sup>6</sup>ASSRC & Institute of Physics and Applied Physics, Yonsei University, 134 Shinchon, Seoul 120-749, Korea

### ABSTRACT

We present angle-resolved photoemission measurements for ultrathin In films on Si(111). Depending on the coverage, this system self-organizes into a metallic monolayer with either  $4\times 1$  or  $\sqrt{7}\times\sqrt{3}$  symmetry relative to the substrate. Electronically, they behave like ideal one- and two-dimensional electron gases (1DEG and 2DEG), respectively. The  $4\times 1$  system has atomic chains of In whose energy bands disperse only parallel to the chains, while for the  $\sqrt{7}\times\sqrt{3}$  system, the dominant reciprocal space features (in both diffraction and bandstructure) resemble a pseudo-square lattice with only weaker secondary features relating to the  $\sqrt{7}\times\sqrt{3}$  periodicity. In both materials the electrons show coupling to the structure. The 1DEG couples strongly to phonons of momentum  $2k_F$ , leading to an  $8\times 2$  Peierls-like insulating ground state. The 2DEG appears to be partially stabilized by electron gap formation at the  $\sqrt{7}\times\sqrt{3}$  zone boundary.

### INTRODUCTION

Owing to the high kinetic energy of free electrons, the metallic state is favored only when the potential energy of the ions dominates this kinetic energy. In this situation, the symmetry of the solid dictates that bands are partially-filled, according to simple, single-particle theory. Many body effects beyond the single electron model can introduce new symmetry breaking factors, which under mean field theory, set in below a critical temperature  $T_c$ . Electrons are removed from the Fermi level, leading to a variety of interesting ground states of metals, of which high- $T_c$  superconductivity in layered perovskites is only one example.

Such many-body effects are often enhanced at low dimensionality because with fewer degrees of freedom, the quasiparticles overlap more and hence interact more readily. Low dimensional metals are therefore interesting for probing how many body effects impact electronic structure, and it is interesting to search for model low-dimensional systems. The most ideal arrangement would be to grow a single monolayer on a semiconducting or insulating substrate in order to eliminate coupling between metal overlayers and the substrate states.

In this paper we report measurements of In on Si(111) self-assembled structures which behave as nearly ideal one and two-dimensional electron gases (1DEGs and 2DEGs). At around one monolayer, the 1DEG is comprised of chains of In atoms in a  $4\times 1$  reconstruction. The 2DEG is the so-called  $\sqrt{7}\times\sqrt{3}$  “rect” phase at coverage just over 1 ML. The films are characterized structurally with low energy electron diffraction (LEED) and x-ray photoelectron diffraction (XPD). The electronic structure is characterized with Fermi surface mapping and

bandmapping. In this technique, soft-x-ray photons induce valence band electrons to be photoemitted into the vacuum where they are detected by an angle- and energy- resolving hemispherical electron spectrometer. Knowing the photon energy and the photoemission angle allows one to determine uniquely the binding energy and momentum of the valence electrons. Angle-resolved photoemission measurements were obtained at beamline 7.0 of the Advanced Light Source in Berkeley, CA. Samples were created by evaporating In onto clean, room-temperature Si  $7\times 7$  wafers, cleaned by resistive direct current heating. Post-growth annealing gives the desired In layer.

### $\sqrt{7\times\sqrt{3}}$ RECONSTRUCTION : 2DEG [1]

Two  $\sqrt{7\times\sqrt{3}}$  reconstructions – pseudo hexagonal (“hex”) and pseudo rectangular (“rect”) were reported by Kraft et al to coexist on the same sample for coverages near one monolayer [2]. In order for us to achieve pure, single domain  $\sqrt{7\times\sqrt{3}}$ -rect samples, we overexposed the samples to In, and then annealed away excess In at  $\sim 300\text{C}$ . The absence of multiple domains, not previously reported, was encouraged through the use of vicinal Si(111) wafers, which were miscut approximately 2 degrees towards the  $[1,1,-2]$  azimuth.

Figure 1a shows the atomic arrangement of the  $\sqrt{7\times\sqrt{3}}$  reconstruction which was determined by Kraft et al. [2]. The  $\sqrt{7\times\sqrt{3}}$  unit cell is populated with 6 In atoms for each of the 5 Si atoms in the underlying  $1\times 1$  unit cells. To a first approximation, the In atoms are arranged in a slightly distorted square lattice similar in dimensions to an isolated In(001) layer. The In atoms within the  $\sqrt{7\times\sqrt{3}}$  unit cell are not equivalent because of the variety of underlying Si bonding geometries. As a result a significant buckling ( $0.75\text{ \AA}$ ) was found in the In atoms. However, to lowest order we can neglect the  $\sqrt{7\times\sqrt{3}}$  superstructure and consider the atoms to lie in a “ $1\times 1$ -rect” lattice. This is distinguished from the underlying, hexagonal Si  $1\times 1$  lattice.

Figure 1b shows the principle LEED diffraction spots to be expected for the three lattices present:  $1\times 1$  (i.e. Si),  $1\times 1$ -rect and  $\sqrt{7\times\sqrt{3}}$ -rect. The particular atomic basis within the  $\sqrt{7\times\sqrt{3}}$  (“hex” or “rect”) could modify the spot intensities through a structure factor. In practice, however, Kraft et al reported the same LEED pattern for both hexagonal and rectangular  $\sqrt{7\times\sqrt{3}}$  polytypes. Figure 1c shows the LEED pattern we obtained. We find the pattern to be dominated

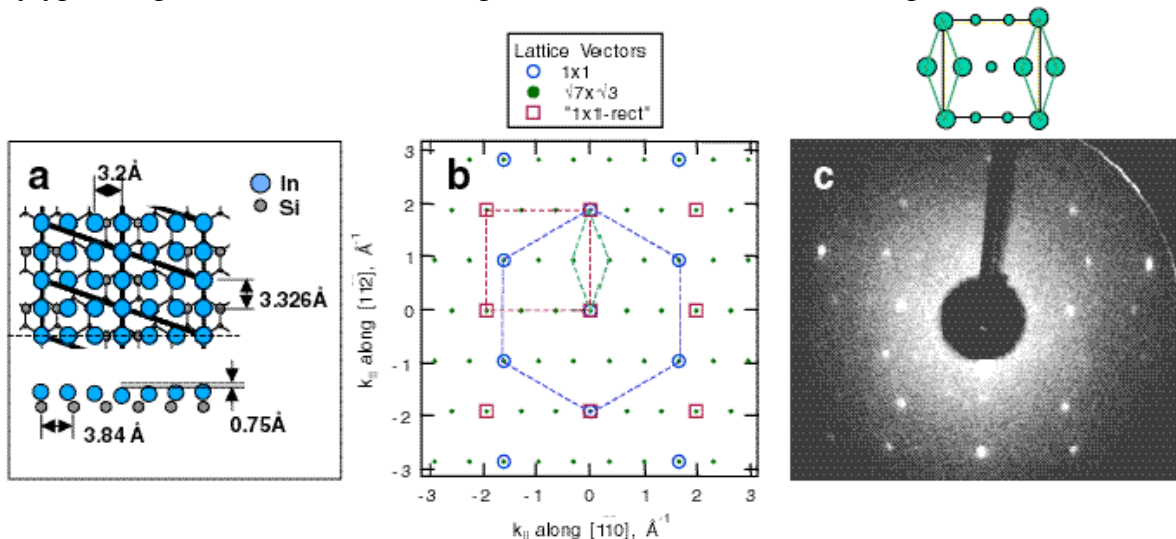


Figure 1. Structural model and diffraction pattern for  $\sqrt{7}\times\sqrt{3}$  In/Si(111). (a) Model proposed by Kraft et al. (b) positions of principle reciprocal lattice points. (c) LEED pattern obtained. The inset shows the unit building block of this pattern; the spot sizes indicate the relative intensity averaged over energy.

by the  $1\times 1$ -rect spots, although all the  $\sqrt{7}\times\sqrt{3}$  spots are showing up in the LEED pattern to a greater or lesser extent. The inset to figure 1c shows a cartoon of the basic building block of the LEED pattern, with circles to indicate the relative spot intensity taken over various beam energies.

In order to distinguish between the rectangular and hexagonal  $\sqrt{7}\times\sqrt{3}$  polytypes, we performed x-ray photoelectron diffraction (XPD) measurements of the In 4d core level. The core-level emission profile reflects the local symmetry near the emitting In atoms. Multiple scattering simulations using the Multiple Scattering Calculation of Diffraction (MSCD) [3] code demonstrate that the observed XPD patterns are not very sensitive to the underlying Si atoms. This is due both to the greater weight of the In nuclei ( $Z=49$ ) compared to Si ( $Z=14$ ) as well as due to the multiplicity of Si bonding sites within the large unit cell. Therefore, the 3-fold symmetric underlying Si geometry should not contribute significantly to the observed XPD patterns. This means that if the resulting XPD pattern has three-fold symmetry, it reflects that the sample has hexagonal symmetry within the In layer, while if the pattern is pseudo 4-fold symmetric then the In layer has local rectangular symmetry. The raw data (figure 2a) shows peripheral rings arranged in a nearly 4-fold symmetry. We have symmetrized the data by 180-degree rotation and enforced mirror plane symmetry to illustrate this point (figure 2b). Although the sample is expected to have 2 mirror planes, in fact the experimental arrangement breaks this mirror plane symmetry, so that features across the mirror planes will have the same positions, but different intensities. Critical comparison of the raw and symmetrized data show no trace

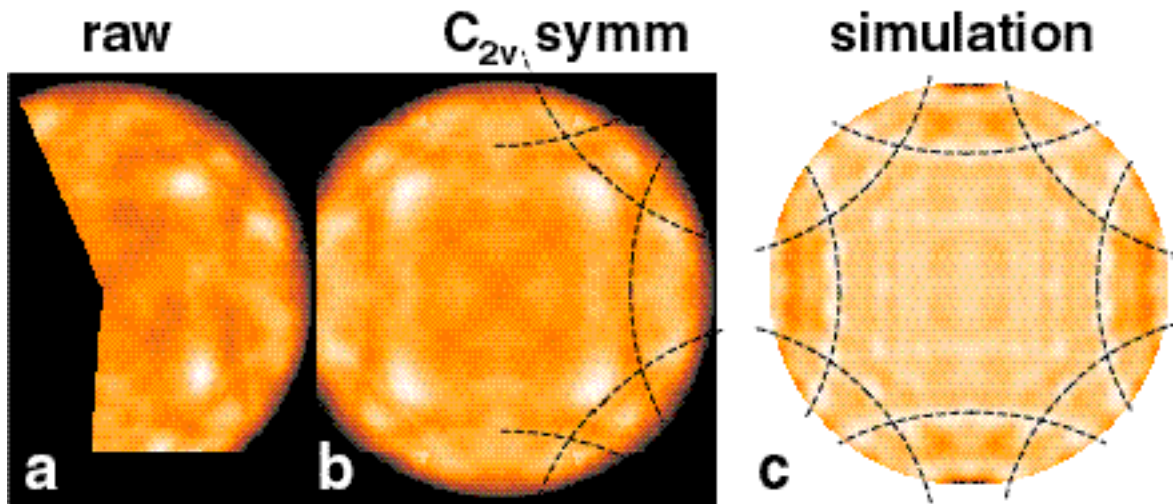


Figure 2. X-ray photoelectron diffraction results for  $\sqrt{7}\times\sqrt{3}$  In/Si(111). (a) Emission profile for In 4d electrons at kinetic energy 185 eV. (b) The same data symmetrized by 180 degree rotation plus mirror plane. (c) Multiple scattering simulation for an unbuckled  $1\times 1$ -rect arrangement of In/Si(111).

whatsoever of 3-fold symmetric features. The dashed lines in figure 2b indicate the principle diffraction rings, which are consistent with two 4-fold NN shells found in a pseudo-square

lattice. Multiple scattering simulations (figure 2c) which were carried out for an unrelaxed square lattice (1x1-rect) are in agreement with the pattern measured with respect to the brightest outer diffraction rings. Much of the remaining fine structure will be sensitive to the detailed  $\sqrt{7}\times\sqrt{3}$  atomic arrangements, which have been left unoptimized in the simulation.

We therefore conclude that we achieved a preparation of a pure, single-domain rectangular  $\sqrt{7}\times\sqrt{3}$  reconstruction. This is fully consistent with the dramatic Fermi surface measurements reported next.

Figure 3a shows a survey of the momentum distribution of the density of states near  $E_F$ . The same data symmetrized in fashion similar to the XPD data is shown in figure 3b, together with the surface Brillouin zone boundaries (BZBs) which are present in the system. We took this data over a larger azimuthal range but with coarser sampling (not shown) in order to verify the correctness of our symmetrization. The most dramatic feature is a more or less square array of very sharp circular contours, which can be simply understood in terms of a trivalent metal on a slightly distorted square lattice (figure 3c). A parabolic nearly free electron band emanates from each  $\Gamma$  point of the reciprocal 1x1-rect lattice. Sampling a constant energy contour at  $E_F$  reveals circular cross sections of these paraboloids. Additional features, which we originally supposed to be caused by the presence of weaker minority domains rotated 120-degrees, can in fact be understood by locating additional parabolic bands centered on the subsidiary  $\sqrt{7}\times\sqrt{3}$  spots found in the LEED pattern, which act as additional  $\Gamma$  points. We only needed to consider the principle LEED spots to account for nearly all of the remaining features (figure 3d). Due consideration

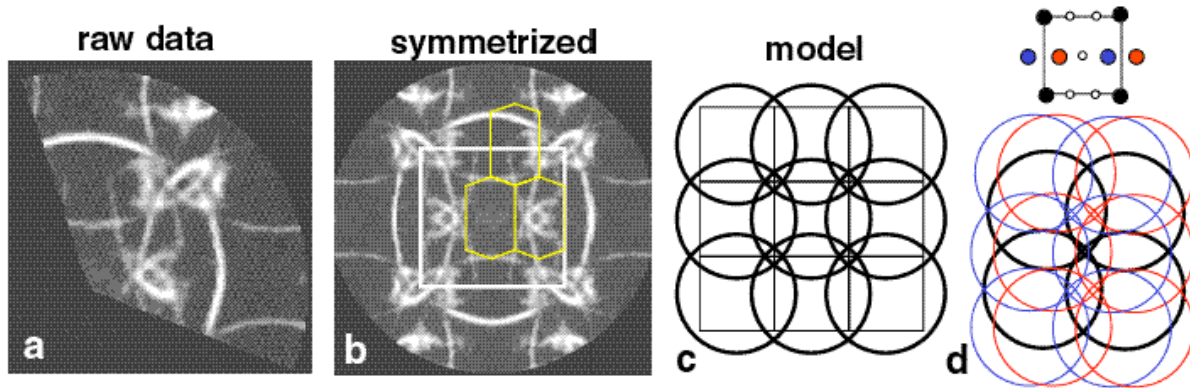


Figure 3. Fermi surface results for  $\sqrt{7}\times\sqrt{3}$  In/Si(111). (a) raw data (b) symmetrized by rotation and mirror planes. (c) Simple model assuming 1x1-rect arrangement of In atoms. (d) model including additional free electron bands centered on  $\sqrt{7}\times\sqrt{3}$   $\Gamma$  points.

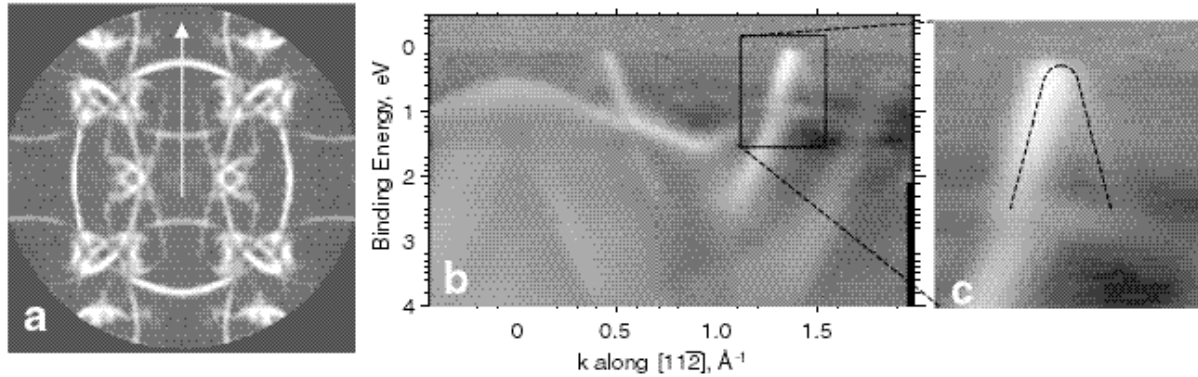


Figure 4. Bandmapping results for  $\sqrt{7}\times\sqrt{3}$  In/Si(111). (a) Fermi surface (b) bandmap at large angle range for the single-arrow in (a), (c) bandmap detail for smaller angle and energy range. The faint backfolded band due to  $\sqrt{7}\times\sqrt{3}$  zone boundary is plainly visible. (Data in (b) and (c) are normalized to Fermi function to improve contrast).

must be placed on the strong matrix element effects, which cause the intensity over most of the subsidiary Fermi contours to be negligible away from the region near the strongest LEED spots

It is noted in Figure 3b that the  $\sqrt{7}\times\sqrt{3}$  BZ boundary happens to align exactly with the Fermi contours along the [1,1,-2] direction. This coincidence suggests that the unusual reconstruction may be partially stabilized by electron energy gap formation as the bands cross the zone boundary. Figure 4 shows bandmapping results for scans along this direction. The backfolded bands from the  $\sqrt{7}\times\sqrt{3}$  symmetry are clearly visible.

#### **4x1 RECONSTRUCTION: 1DEG [4]**

Further annealing of the  $\sqrt{7}\times\sqrt{3}$ -rect sample at about 600K leads to formation of single-domain 4x1 reconstructed In on Si(111). This system was characterized structurally [5-9] and electronically [10,11]. In these works it was found that the In atoms were organized into linear chains of atoms, and that the electronic properties appeared to be highly anisotropic, with metallic behavior indicated by band crossings of  $E_F$  along the chains. A detailed structure analysis by x-ray scattering was recently published [12].

Because of the inherent instability of one-dimensional metals, we examined the structure and electronic properties of the 4x1 reconstruction at low temperature. Figure 5 shows reflection high-energy electron diffraction (RHEED) patterns for (a) the room temperature (RT) 4x1 phase and (b) at low temperature (100K, LT). The latter shows a period doubling of the x1 direction indicated by the formation of streaks in the x2 position. Additional weak spots in the 4x direction are also indicated in figure 5b. This means that the low temperature phase has 8x “2” symmetry, which indicates some coupling of the structures between adjacent metallic chains. (The quoted “2” indicates the streakiness of the x2 features).

That the low-temperature phase has period-doubling along the metal chains is compatible with a metal-to-insulator transition with a Peierls-like mechanism. The Peierls metal-to-insulator transition occurs because of the relative energy gain due to gap formation when a one-dimensional lattice is slightly distorted from its equilibrium (without electron-phonon coupling) lattice constant. For an exactly half-filled band, a lattice distortion consisting of doubling the



lattice constant suffices to create a new BZB at the Fermi level crossing. The electronic gap formation induced by this spontaneous symmetry change stabilizes the distortion, which occurs below a critical temperature according to mean field theory [13]. In order to prove that this

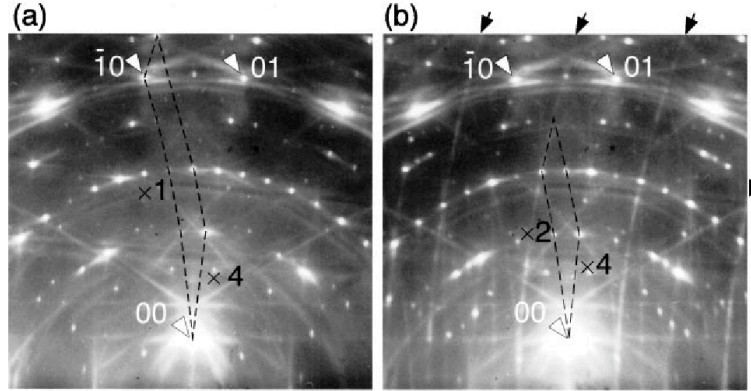


Figure 5. Reflection high-energy electron diffraction patterns for (a) the room-temperature  $4 \times 1$  phase and (b) the  $4 \times '2'$  unit cells are depicted by dashed lines, and the streaks due to periodicity doubling ( $\times 2$ ) along the linear chain direction at  $\sim 100\text{K}$  are indicated by the arrows.

mechanism occurs, it is necessary to establish: (i) the symmetry change (e.g.  $x1 \rightarrow x2$  symmetry), (ii) that there exists an exactly half-filled band, and (iii) that the material becomes insulating at LT.

In order to examine these issues in further detail, we performed high-resolution STM microscopy of the two phases, which are presented in Figure 6 for (a) RT and (b) LT. Clear period doubling along the chains is evident between these two images. In our interpretation, the bright features in figure 2b are charge density wave (CDW) modulations associated with the Peierls-distorted ground state. Some correlations of the CDW modulations between chains are apparent, however, supporting the idea that the system is not perfectly one-dimensional. For example, CDW oscillations tend to be locked in phase between adjacent wires. Nevertheless, the coupling is weak, indicated by significant numbers of out-of phase CDW between wires, as well as some quickly fluctuating CDW, as indicated in figure 6b.

It was suggested in the earlier electronic studies that the system was metallic with a high degree of asymmetry [10,11], and that furthermore there existed a half-filled band [11]. Our measurements are precise enough to determine the exact band filling, as well as the degree of coupling between the chains from the bandstructure. In figure 7, we present RT momentum distribution (MD) patterns in  $k$ -space for electrons at the Fermi level  $E_F$ . Figure 7(a) shows a wide view of the MD pattern, indicated on the right side a series of more-or-less uniformly vertical features. These correspond to the Fermi crossings of underlying bands, labelled  $m_1$ ,  $m_2$ ,  $m_3$  following the convention of Ref. [11]. Figure 7(b) shows a detailed view of the Fermi contours. It is evident that of these, state  $m_2$  is perfectly straight (and hence perfectly one-dimensional) within the accuracy of our measurement ( $\sim 0.02 \text{ \AA}^{-1}$ ). The other two states,  $m_1$  and  $m_3$ , are not perfectly straight, and therefore represent states whose wavefunctions have some overlap between adjacent metal chains.

In addition to establishing the one-dimensionality of the  $m_3$  electronic state, we also demonstrated that this band is half-filled. The double arrow in figure 7a (“nesting” vector) represents the change in momentum ( $2k_F$ ) when an electron is transferred from one  $m_3$  Fermi

contour to another across the Brillouin Zone (BZ). That this arrow has length exactly half the BZ width ( $=\pi/a$ ) is exactly equivalent to saying the band is half-filled.

So the In/Si(111)  $4 \times 1$  at least partially meets the criteria discussed above for a Peierls-like transition. It is furthermore desirable to show that the material becomes partially or fully insulating at low temperature. So far there are two attempts to demonstrate this. Angle-resolved photoemission measurements indicated at least partial (pseudo-) gap formation due to a Peierls-like mechanism [4]. And more recently, high-resolution electron energy loss spectroscopy shows a significant decrease in the metallicity at low temperature. [14]

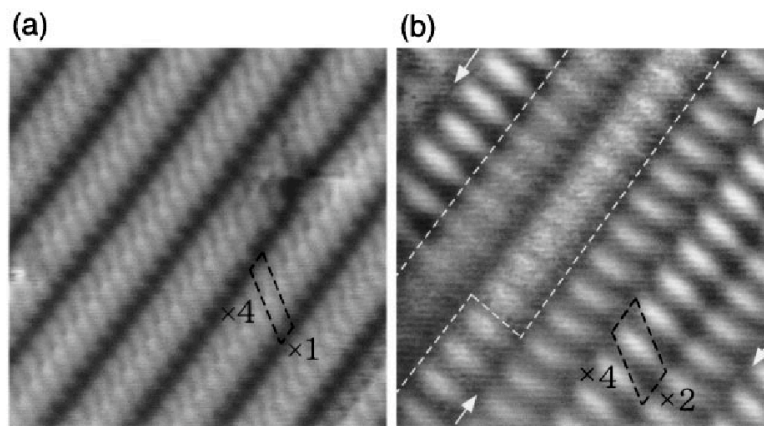


Figure 6. Scanning tunneling microscopy images of (a) room temperature  $4 \times 1$  phase and (b) the low-temperature ( $\sim 65$  K)  $4 \times '2'$  phase were taken at the same sample bias voltage of  $\sim 1$  V (filled state) in the constant-height mode. The  $4 \times 1$  and  $4 \times 2$  unit cells are indicated by black dashed lines. The area of the characteristic fluctuating charge-density region (white dashed lines) and the phase mismatching between the neighboring chains (arrows) are observed.

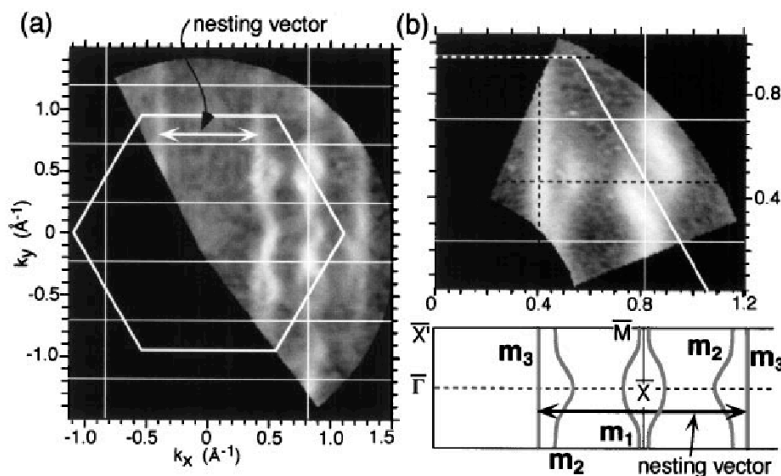




Figure 7. (a) Fermi surface plot for the room temperature  $4 \times 1$  phase obtained by angle resolved photoemission (at photon energy  $h\nu = 85$  eV) and (b) its details for an irreducible part of the surface Brillouin zone with a schematic of the Fermi contours determined. The  $1 \times 1$  and  $4 \times 1$  surface Brillouin zones are depicted with thick and thin solid lines, resp., where a rectangular  $4 \times 1$  Brillouin zone is taken for clarity. The arrows indicate the distance from  $m_1$  to  $m_3$  bands across the unit cell, which is exactly half the unit cell dimension (indicating half-filled bands).

## SUMMARY AND OUTLOOK

To summarize, we have found that pure, single-domain one and two-dimensional metallic In can be prepared on Si(111) substrates. These materials have signatures of nearly ideal one and two-dimensional electron gases. The higher coverage, two-dimensional  $\sqrt{7} \times \sqrt{3}$  In on Si(111) system has local pseudo-4-fold symmetry, and its electronic structure is dominated by the potential energy distribution of a slightly distorted square (“ $1 \times 1$ -rect”) lattice. Nevertheless, the external potential of the substrate atoms has some effect on the electronic structure and indeed the interplay between the periodicities ( $1 \times 1$ -rect and  $\sqrt{7} \times \sqrt{3}$ ) may contribute to the stability of the system. The lower-coverage  $4 \times 1$  reconstruction was also found to have an interplay between electronic properties and its structure. Evidence for a Peierls-like instability was presented based on STM, diffraction, and Fermi surface mapping.

One of the enduring motivations to study low-dimensional metals is the fact that the many-body effects are greatly enhanced compared to three-dimensional metals. One such effect, electron-phonon coupling, was highlighted here, since it leads to Peierls-like distortion of one-dimensional metals and greatly altered electronic ground state. More exotic ground states are also possible, such as two-dimensional superconductivity, etc. Indeed, many of the most interesting materials today, such as high-temperature superconductors, colossal magnetoresistance materials, etc. are comprised of two-dimensional layers whose electronic states determine their novel electronic properties. Therefore, it is interesting to identify model low-dimensional systems in order to probe their properties. Of the systems measured so far, low-dimensional metals on Si offer a very promising route to this goal. One of the main advantages offered are the lack of bulk states to scatter into, so that the low-dimensionality is not destroyed by scattering into nearby bulk states. In this work, we presented just two examples, but in fact many metals on Si are known to make similar structures, and their electronic properties have only been partially studied so far.

This work was supported by the Department of Energy under grant DE-FG06-86ER45275, and was performed at the Advanced Light Source at the Ernest Orlando Lawrence Berkeley National Laboratory.

## REFERENCES

1. E. Rotenberg, H. W. Yeom, J. H. Schaefer, B. Krenzer, M. Rocha, and S. D. Kevan, to be published.
2. J. Kraft, S. L. Surnev, and F. P. Netzer, *Surface Science* **340**, 36 (1995).
3. Yufeng Chen and M. A. v. Hove, <http://electron.lbl.gov/mscdpack>.

4. H. W. Yeom, S. Takeda, E. Rotenberg, I. Matsuda, K. Horikoshi, J. Schaefer, C. M. Lee, S. D. Kevan, T. Ohta, T. Nagao, and S. Hasegawa, *Phys. Rev. Lett.* **82**, 4898 (1999).
5. V. G. Lifshits, *Surface Phases on Silicon: Preparation, Structure, and Properties* (Wiley, Chichester, 1994).
6. J. Nogami, S. I. Park, and C. F. Quate, *Phys. Rev. B* **36**, 6221 (1987).
7. A. A. Saranin, A. V. Zotov, K. V. Ignatovich, V. G. Lifshits, T. Numata, O. Kubo, H. Tani, M. Katayama, and K. Oura, *Phys. Rev. B* **56**, 1017 (1997).
8. T. Abukawa, F. Hisamatsu, M. Nakamura, S. Kono, T. Goto, M. Sasaki, T. Kinoshita and A. Kakizaki, *J. Electron Spectrosc. Relat. Phenom.* **80**, 233 (1996).
9. C. Collazo-Davila, L. D. Marks, K. Nishii, Y. Tanishiro, *Surf. Rev. Lett.* **4**, 65 (1997).
10. I. G. Hill and A. B. McLean, *Phys. Rev. B* **56**, 15725 (1997); **59**, 979 (1999).
11. T. Abukawa, M. Sasaki, F. Hisamatsu, T. Goto, T. Kinoshita, A. Kakizaki, S. Kono, *Surf. Sci.* **325**, 33 (1995).
12. O. Bunk, G. Falkenberg, J. H. Zeysing, L. Lottermoser, R. L. Johnson, M. Nielsen, F. Berg-Rasmussen, J. Baker, and R. Feidenhans'l, *Phys. Rev. B* **59**, 12228 (1999).
13. G. Grüner, *Density Waves in Solids*, (Addison Wesley, 1994).
14. K. Sakamoto, H. Ashima, H. W. Yeom, and W. Uchida, *Phys. Rev. B* **62**, 9923 (2000).